Current Research in Parasitology & Vector-Borne Diseases 1 (2021) 100041

Contents lists available at ScienceDirect

Current Research in Parasitology & Vector-Borne Diseases

journal homepage: www.editorialmanager.com/crpvbd/default.aspx

Towards understanding transfluthrin efficacy in a pyrethroid-resistant strain of the malaria vector *Anopheles funestus* with special reference to cytochrome P450-mediated detoxification

Melanie Nolden [a,b], Andreas Brockmann [a,c], Ulrich Ebbinghaus-Kintscher [a], Kai-Uwe Brueggen [a], Sebastian Horstmann [a], Mark J.I. Paine [b], Ralf Nauen [a,*]

[a] Bayer AG, Crop Science Division, Alfred Nobel Str. 50, D-40789, Monheim am Rhein, Germany
[b] Department of Vector Biology, Liverpool School of Tropical Medicine, Pembroke Place, Liverpool, L3 5QA, United Kingdom
[c] Rheinische Friedrich-Wilhelms-Universität Bonn, D-53113, Bonn, Germany

ARTICLE INFO

Keywords:
Anopheles
Pyrethroid resistance
P450
Synergists
Azole fungicides
Sodium channel
Deltamethrin
FUMOZ-R
Malaria

ABSTRACT

Malaria vector control interventions rely heavily on the application of insecticides against anopheline mosquitoes, in particular the fast-acting pyrethroids that target insect voltage-gated sodium channels (VGSC). Frequent applications of pyrethroids have resulted in resistance development in the major malaria vectors including *Anopheles funestus*, where resistance is primarily metabolic and driven by the overexpression of microsomal cytochrome P450 monooxygenases (P450s). Here we examined the pattern of cross-resistance of the pyrethroid-resistant *An. funestus* strain FUMOZ-R towards transfluthrin and multi-halogenated benzyl derivatives, permethrin, cypermethrin and deltamethrin in comparison to the susceptible reference strain FANG. Transfluthrin and two multi-fluorinated derivatives exhibited micromolar potency - comparable to permethrin - to functionally expressed dipteran VGSC in a cell-based cation influx assay. The activity of transfluthrin and its derivatives on VGSC was strongly correlated with their contact efficacy against strain FUMOZ-R, although no such correlation was obtained for the other pyrethroids due to their rapid detoxification by the resistant strain. The low resistance levels for transfluthrin and derivatives in strain FUMOZ-R were only weakly synergized by known P450 inhibitors such as piperonyl butoxide (PBO), triflumizole and 1-aminobenzotriazole (1-ABT). In contrast, deltamethrin toxicity in FUMOZ-R was synergized > 100-fold by all three P450 inhibitors. The biochemical profiling of a range of fluorescent resorufin and coumarin compounds against FANG and FUMOZ-R microsomes identified 7-benzyloxymethoxy-4-trifluoromethylcoumarin (BOMFC) as a highly sensitive probe substrate for P450 activity. BOMFC was used to develop a fluorescence-based high-throughput screening assay to measure the P450 inhibitory action of potential synergists. Azole fungicides prochloraz and triflumizole were identified as extremely potent nanomolar inhibitors of microsomal P450s, strongly synergizing deltamethrin toxicity in *An. funestus*. Overall, the present study contributed to the understanding of transfluthrin efficacy at the molecular and organismal level and identified azole compounds with potential to synergize pyrethroid efficacy in malaria vectors.

1. Introduction

The annual infection of humans with malaria remains high with an estimated 219 million cases and 435,000 deaths worldwide in 2017 (WHO, 2018a), the majority (~80%) occurring in sub-Saharan Africa. In Africa malaria is primarily transmitted by sibling species from the Gambiae complex such as *Anopheles gambiae* and *An. arabiensis*, and *An. funestus* (Diptera: Culicidae) from the Funestus subgroup (Sinka et al., 2010; Wiebe et al., 2017). *Anopheles funestus* is one of the major malaria vectors in sub-Saharan-Africa (Temu et al., 2007; Sinka et al., 2010), but its predicted geographical occurrence differs from *An. gambiae* (Wiebe et al., 2017).

Vector control interventions targeting anopheline mosquitoes mainly rely on long-lasting insecticidal nets (LLINs) or indoor residual sprays (IRS) (Bhatt et al., 2015; Sinka et al., 2016), using longstanding chemical classes of insecticides addressing a few modes of action (Nauen, 2007; Hoppé et al., 2016). For over 50 years adult mosquito control has relied on four different chemical classes of insecticides, i.e. DDT,

* Corresponding author.
E-mail address: ralf.nauen@bayer.com (R. Nauen).

https://doi.org/10.1016/j.crpvbd.2021.100041
Received 24 May 2021; Received in revised form 23 June 2021; Accepted 13 July 2021

organophosphates, carbamates and pyrethroids, addressing two modes of action. This contrasts with a much larger arsenal of insecticides targeting a much wider range of modes of action that are available for the control of agricultural pest species (Hemingway et al., 2006; Nauen, 2006; Sparks and Nauen, 2015). It is only very recently that the neonicotinoid clothianidin was introduced, an agricultural pesticide with a new mode of action for vector control uses either alone or in combination with a pyrethroid (Fuseini et al., 2019; Fongnikin et al., 2020).

The success of pyrethroids as insecticides such as deltamethrin (Pulman, 2011) is mainly based on their broad activity against a diverse range of pests and their fast knock-down action (Soderlund, 2020) resulting from the modulation of voltage-gated sodium channels (VGSC) in the insects' central nervous system (Field et al., 2017; Scott, 2019). Pyrethroids are broadly divided into two classes designated as type-I and type-II pyrethroids (Soderlund, 2020), based on the respective absence and presence of an α-cyano substituent that increases VGSC potency that determines the evoked physiological responses (Casida et al., 1983; Laufer et al., 1984; Soderlund and Bloomquist, 1989). Pyrethroids as insecticide sprays for vector control were introduced in the early 1970's (permethrin) and remained the cornerstone for vector control through the introduction of pyrethroid treated bednets 20 years ago, an intervention amongst others contributing to a significant decline in clinical cases of malaria between 2000 and 2015 (Bhatt et al., 2015). However, the spatially expanded exposure of anopheline mosquitoes to pyrethroids in impregnated bednets (ITNs) and LLINs, resulted in an increasing selection of alleles conferring resistance (Coleman et al., 2017; WHO, 2018b; Moyes et al., 2020). Therefore, the efficacy of these control measures is increasingly compromised by the development and spread of pyrethroid resistance alleles in anopheline mosquitoes, including *An. funestus* (Hemingway et al., 2016; Coleman et al., 2017; Hemingway, 2019).

Two major mechanisms have been described to confer pyrethroid resistance in anopheline mosquitoes (Hemingway et al., 2004; Coleman et al., 2017); metabolic resistance, in particular detoxification mediated by elevated levels of microsomal cytochrome P450 monooxygenases (P450s) (Vontas et al., 2020) known to be involved in oxidative metabolism of xenobiotics (Feyereisen, 1999), and target-site mutations resulting in decreased affinity of pyrethroids to their site of binding in VGSC due to amino acid substitutions, also called knock-down resistance (kdr) (Davies et al., 2007; Scott, 2019; Smith et al., 2019). Other mechanisms such as changes in cuticular hydrocarbons - resulting in decreased penetration of pyrethroids - are factors shown to contribute to resistance (Balabanidou et al., 2018).

Pyrethroid resistance in *An. funestus* was first described in South Africa (Hargreaves et al., 2000) and shown to be synergized by piperonyl butoxide (PBO), an inhibitor of P450 enzymes (Brooke et al., 2001). Bednets co-impregnated with PBO and pyrethroids were only recently endorsed to mitigate the effects of P450 associated resistance (Gleave et al., 2018; Moyes et al., 2020). Interestingly, despite high levels of pyrethroid resistance in *An. funestus* VGSC mutations known to confer kdr have not yet been described (Irving and Wondji, 2017), whilst kdr has become essentially fixed in populations of *An. gambiae* (Coetzee and Koekemoer, 2013). Upregulated levels of P450s linked to pyrethroid resistance in *An. funestus* have been reported in many field studies in Africa (Cuamba et al., 2010; Morgan et al., 2010; Irving et al., 2012; Djouaka et al., 2016; Sangba et al., 2016; Tchigossou et al., 2018). The genetically duplicated and highly overexpressed P450 alleles CYP6P9a and CYP6P9b are key determinants of pyrethroid-resistance in *An. funestus* (Wondji et al., 2009; Riveron et al., 2013), that have been shown to compromise the efficacy of pyrethroid-treated bednets (Weedall et al., 2019). Many laboratory studies were conducted with the field-collected *An. funestus* colony FUMOZ, especially strain FUMOZ-R, a laboratory-selected reference strain expressing high levels of P450-mediated pyrethroid resistance and lacking kdr (Coetzee and Koekemoer, 2013). It was also shown that cuticle thickening in *An. funestus* (FUMOZ) could apparently affect pyrethroid penetration and thus contributing as an adjunct to the primary mechanism of resistance based on P450 overexpression (Wood et al., 2010).

Not all pyrethroids are similarly affected by P450-mediated resistance in *An. funestus* as recently demonstrated for the multi-halogenated benzyl pyrethroid transfluthrin (Horstmann and Sonneck, 2016). Transfluthrin (2,3,5,6-tetrafluorobenzyl(1R,3S)-3-(2,2-dichlorovinyl)-2,2-dimethylcyclo-propanecarboxylate; syn. benfluthrin) is an enantiomerically pure and volatile pyrethroid exhibiting spatial repellent activity against mosquitoes (Ogoma et al., 2012, 2014; Bibbs et al., 2018). It is under scrutiny as a complementary outdoor-protection tool to current vector control interventions (Kline and Urban, 2018; Masalu et al., 2020).

Here, we have examined the cross-resistance pattern of transfluthrin and halogenated benzyl derivatives against a susceptible strain (FANG) and the FUMOZ-R pyrethroid-resistant strain of *An. funestus*. We have also measured the interactions of pyrethroids with recombinantly expressed dipteran VGSC and explored the role of microsomal P450s in transfluthrin metabolism and resistance by synergist studies *in vivo* and *in vitro*. Overall, this has provided new insights on the efficacy and resistance-breaking properties of transfluthrin in pyrethroid-resistant *An. funestus* that will aid the development of new malaria control products.

2. Materials and methods

2.1. Mosquito strains

Anopheles funestus FUMOZ-R strain was obtained in 2011 from the National Institute for Communicable Diseases - Vector Control Reference Unit (VCRU) (Johannesburg, South Africa) and maintained at Bayer AG (Monheim, Germany) without insecticide selection pressure. It was originally collected in 2000 in South Mozambique and is highly resistant to pyrethroids (Brooke et al., 2001; Hunt et al., 2005), driven by the overexpression of cytochrome P450 monooxygenases (P450s) (Amenya et al., 2008). The insecticide susceptible *An. funestus* FANG strain was obtained in 2019 from the Liverpool Insecticide Testing Establishment (LITE) at the Liverpool School of Tropical Medicine (LSTM). The strain was originally received from the National Institute for Communicable Diseases (NICD) in South Africa and collected in Angola. Both strains were kept at 27.5 ± 0.5 °C, 65 ± 5% relative humidity and a photoperiod of 12/12 L:D with 1-h dusk/dawn. Adults were kept in rearing cages (46 cm × 33 cm × 20 cm) and five days after hatching the first blood meal (bovine blood, obtained from Elocin Laboratory, Oberhausen, Germany) was provided according to standard protocols (Das et al., 2007; Human Disease Vectors (HDV) group of the Insect Pest Control Laboratory, 2017).

2.2. Chemicals

Transfluthrin (CAS: 118712-89-3), deltamethrin (CAS: 52918-63-5), permethrin (CAS: 52645-53-1), 1-aminobenzotriazole (1-ABT) (CAS: 1614-12-6), triflumizole (CAS: 68694-11-1) and piperonyl butoxide (PBO) (CAS: 51-03-6) were obtained from Sigma-Aldrich/Merck (Darmstadt, Germany) of the highest purity available. Cypermethrin, and the transfluthrin derivatives TF-0, TF-1, TF-3 and TF-5 (Fig. 1) were of analytical grade and obtained internally from Bayer (Leverkusen, Germany). TF-5 is also known as fenfluthrin (Behrenz and Elbert, 1985). Transfluthrin is an enantiomerically pure compound (> 98% 1R-trans; < 1.0% 1S-trans). A similar enantiomeric purity is expected for the transfluthrin derivatives, which were synthesized starting from reactions of optically active 1R-trans-permethric acid chloride with the respective halogenated benzyl alcohol as described elsewhere (Naumann, 1990).

β-Nicotinamide adenine dinucleotide 2′-phosphate (NADPH) reduced tetrasodium salt hydrate (CAS: 2646-71-1 anhydrous, purity ≥ 93%), 7-ethoxycoumarin (EC; CAS: 31005-02-4, purity > 99%), 7-methoxy-4-trifluoromethylcoumarin (MFC; CAS: 575-04-2, purity ≥ 99%), 7-Ethoxy-4-trifluoromethylcoumarin (EFC; CAS: 115453-82-2, purity ≥ 98%) 7-benzyloxy-4-trifluoromethylcoumarin (BFC; CAS: 220001-53-6,

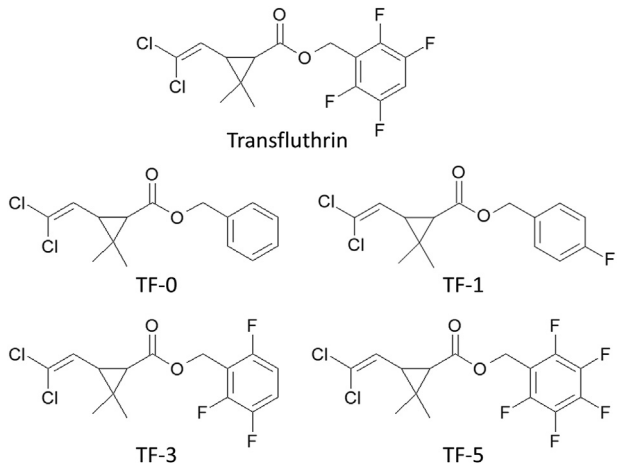

Fig. 1 Chemical structures of transfluthrin and its derivatives used in this study.

purity ≥ 99%), 7- hydroxy-coumarin (HC; CAS: 93-35-6, purity 99%) 7-hydroxy-4-trifluoromethylcoumarin (HFC; CAS: 575-03-1, purity 98%), 7-methoxyresorufin (MR; CAS: 5725-89-3, purity ≥ 98%), 7-ethoxyresorufin (ER; CAS: 5725-91-7, purity ≥ 95%), 7-benzoxyresorufin (BR; CAS: 87687-02-3), 7-n-pentoxyresorufin (PR; CAS: 87687-03-4) and resorufin sodium salt (CAS: 34994-50-8) were purchased from Sigma-Aldrich/Merck (Darmstadt, Germany). 7-Benzyloxymethoxy resorufin (BOMR; CAS: 87687-02-3; Vivid™ P2951) was purchased from Invitrogen, Thermo Fisher Scientific, Waltham, USA. 7-benzyloxymethoxy-4-trifluoromethylcoumarin (BOMFC; CAS: 277309-33-8; purity 95%) was synthesized by Enamine (Riga, Latvia). All chemicals were of analytical grade unless otherwise stated.

2.3. Glazed tile bioassay

To generate dose-response curves of pyrethroids, *An. funestus* FANG and FUMOZ-R mosquitoes were exposed to a range of different concentrations in a glazed tile assay as recently described by Horstmann and Sonneck (2016). Briefly: three to five days-old mosquitoes were anesthetized by placing them for 1 min at −20 °C and afterwards on a cooling plate at 2 °C. Ten females were placed in a Petri dish (diameter: 5 cm; height: 1 cm, including 12 ventilation holes) covered with a paper card. Insecticides were dissolved in acetone with a starting concentration of 2,000 ppm (equal to 100 mg/m^2) and diluted in 1:5 steps to 0.0256 ppm/0.00512 ppm (0.00128/0.000256 mg/m^2). Using an Eppendorf pipette 1,125 µl of each concentration was applied onto a glazed tile (15 cm × 15 cm, ceramic, Vitra, Germany). After the evaporation of acetone and mosquito recovery from anaesthetation (1 h), mosquitoes were exposed in two replicates ($n = 10$) for 30 min to each insecticide concentration and afterwards transferred back to the untreated paper card and kept in Petri dishes overnight. A 10% dextrose solution was provided overnight as a food source. Mortality was scored 24 h post-exposure. Acetone alone served as a control. Control mortality between 5 and 20% was corrected using Abbott's formula (Abbott, 1925), and bioassays exceeding 20% control mortality were considered invalid. All bioassays were replicated at least five times with two replicates ($n = 10$) unless otherwise stated.

2.4. Synergist bioassays

Final synergist concentrations of PBO, 1-ABT and triflumizole were chosen based on pre-assays assessing the toxicity of each P450 inhibitor by exposing adults of both strains for 30 min to a range of concentrations (10,000; 7,500; 5,000; 4,000; 2,000; 1,000; 500; and 250 ppm in acetone) in a glazed tile assay as described above. After 24 h, the mortality was evaluated. For the final bioassays the following concentrations were chosen: 2,000 ppm (100 mg/m^2) of triflumizole and PBO, and 5,000 ppm (250 mg/m^2) of 1-ABT for strain FUMOZ-R; 500 ppm (25 mg/m^2) of triflumizole and PBO, and 1,000 ppm (50 mg/m^2) of 1-ABT for strain FANG. Final synergist concentrations were applied onto glazed tiles as described above. Ten female adults were exposed for 30 min to each synergist and immediately afterwards transferred to pyrethroid treated glazed tiles as described above. As a control group, mosquitoes which were not exposed to the synergist and completely untreated mosquitoes were included. Mortality figures were corrected according to Abbott (1925), and tests exceeding 20% control mortality were considered invalid. All synergist bioassays were replicated at least twice.

2.5. UPLC-MS/MS analysis

As the synergists were applied *via* tarsal contact, ultra-performance liquid chromatography and mass spectrometry (UPLC/MS) was used to confirm their uptake by exemplarily analyzing exposed FUMOZ-R mosquito adults. PBO (2,000 ppm), triflumizole (2,000 ppm) and 1-ABT (5,000 ppm) were dissolved in acetone and applied onto a glazed tile as described above. After acetone evaporation (1 h) 10 female FUMOZ-R adults were exposed for 30 min to each synergist in replicates ($n = 2$). After exposure, mosquitoes were placed onto a cooling plate (2 °C) to separate legs and mosquito bodies. Legs and body fractions of ten mosquitoes were pooled ($n = 20$) in a 1.5 ml reaction tube, washed five times in 1,100 µl acetonitrile/water (80/20) and subsequently grinded using a micro-pestle in 1100 µl acetonitrile/water (80/20). The samples were centrifuged at 12,000× *g* for 10 min at room temperature (Centrifuge 5418R, Eppendorf, Hamburg, Germany) and the supernatant was transferred into a glass vial for subsequent UPLC-MS/MS analysis with slight modifications according to a previously published protocol (Manjon et al., 2018). Briefly, for the chromatography on an Agilent 1290 Infinity II, a Waters Acquity HSS T3 column (2.1 × 50 mm, 1.8 mm) with 0.025% formic acid in acetonitrile and 0.02% formic acid in water as the eluent in gradient mode was employed. After positive electrospray ionization, ion transitions were recorded on a Sciex API6500 Triple Quad. PBO, triflumizole and 1-ABT were measured in positive ion mode (ion transitions: PBO 356 > 177, triflumizole 346 > 278, 1-ABT 135 > 90.9). The peak integrals were calibrated externally against a standard calibration curve. The linear range for the quantification of PBO, triflumizole, and 1-ABT was 0.25–75 ng/ml, 0.25–100 ng/ml, and 0.5–1,000 ng/ml, respectively. Samples were diluted prior to measurement if needed. Recovery rates of mosquitoes exposed to the chosen synergist concentrations and acetone only were normally close to 100%.

2.6. Voltage-gated sodium channel measurements

The intrinsic potential of transfluthrin, its derivatives and common pyrethroids were measured in a HEK293 cell line expressing para-type voltage-gated sodium channels of *Musca domestica* (GenBank: AAB47604.1) using a Fluorescent Imaging Plate Reader, FLIPR Tetra (Molecular Devices, San Jose, CA, USA) fluorescence-based membrane potential assay (Molecular Devices, #R8034). Cells were plated at a density of 40,000 cells/well two days prior to the assay on black poly-D-lysine coated µClear 384-well plates (Greiner Bio-One, Essen, Germany), incubated overnight at 37 °C (5% CO_2) and subsequently stored 24 h at 26 °C. The FLIPR voltage membrane potential sensitive (MPs) dye assay was conducted with slight modifications according to Tay et al. (2019). Cell medium was removed, and cells were incubated for 1 h with 20 µl per well Tyrode buffer (Sigma T2397) containing 0.01% brilliant black (CAS: 2519-30-4) and 0.75 mg/ml MPs dye in the dark. Common pyrethroids and transfluthrin derivatives were pre-diluted in DMSO and further diluted to a final assay concentration of 50–0.0032 µM (deltamethrin: 50–0.0000256 µM; cypermethrin 10–0.00064 µM) in Tyrode buffer containing 0.03% Pluronic™ F-68 (Thermo Fisher Scientific,

Waltham, USA) (final DMSO concentration: 0.5%). Five µl of each concentration was added to each well and replicated four times and immediately measured every 5 s using the FLIPR high throughput cellular screening system at an emission wavelength of 565–625 nm while excited at 510–545 nm. Maximal response-over-baseline of each kinetic was subjected to further analysis using GraphPad Prism 8.4 (GraphPad Software, San Diego, USA). The assay was repeated three times on different days.

2.7. Isolation of microsomes and cytochrome P450 activity assays

Thirty to fifty adult mosquitoes (FUMOZ-R or FANG) were homogenized in an Eppendorf tube (2 ml) with a micro pestle in 500 µl homogenization-buffer (0.1 M K_2HPO_4, 1 mM DTT, 1 mM EDTA, 200 mM saccharose, pH 7.6) on ice and afterwards centrifuged at 5,000× *g* at 4 °C for 5 min. The supernatant was centrifuged again for 20 min at 15,000× *g* and 4 °C. The resulting supernatant was centrifuged for 1 h at 100,000× *g* and 4 °C (Beckman Coulter, Germany; Optima MAX-XP Benchtop Ultracentrifuge, rotor: MLA 130) and the microsomal pellet was resuspended in 250 µl 0.1 M buffer (0.1 M K_2HPO_4, 1 mM DTT, 0.1 mM EDTA, 5% glycerol, pH 7.6). The protein amount was determined according to Bradford (1976) and adjusted to 0.2 mg protein/ml.

The activity of microsomal monooxygenases was measured using a fluorescent probe assay with different model substrates at 20 ± 1 °C. Depending on the substrate, the final assay concentrations of fluorescence probes were 100 µM (PC), 50 µM (BFC, EC, EFC, MFC), 10 µM (BOMFC) and 4 µM (BOMR, BR, ER, MR, PR) adapted from Zimmer et al. (2014) and Manjon et al. (2018). Substrate stock solutions were prepared in DMSO at 100 mM (PC), 50 mM (BOMFC, BFC, EC, EFC, MFC), 2 mM (BOMR) and 1 mM (BR, ER, MR), and then diluted to the respective concentration with 0.1 M potassium-phosphate buffer (pH 7.6). Twenty-five µl of diluted substrate solution plus 25 µl of diluted enzymes were incubated for 1 h with and without 250 µM NADPH in a black 384-well plate (Greiner bio-one, F-bottom, PS). The reaction was replicated four times and stopped by adding 50 µl of red-ox mix (25% DMSO, 50 mM Tris–HCl buffer (pH 10), 5 mM glutathione oxidized, and 0.2 U glutathione reductase). Fluorescence was evaluated using a microplate reader (Tecan, Spark) at the respective excitation and emission wavelengths as described by Zaworra and Nauen (2019). As a positive control, rat liver microsomes (20 mg protein/ml; Sigma-Aldrich) were tested. The resulting reaction products, i.e. HC, HFC and resorufin were used to generate standard curves to calculate the amount of the respective product in pmol per mg/min (Ullrich and Weber, 1972; Manjon et al., 2018).

2.7.1. Michaelis-Menten kinetics of BOMFC O-dearylation by mosquito microsomes

Substrate concentration dependent microsomal monooxygenase kinetics was evaluated using eleven different BOMFC concentrations (stock 100 mM in DMSO) between 200 µM and 0.195 µM diluted in 0.1 M potassium-phosphate buffer (pH 7.6) containing 0.01% zwittergent 3-10 (CAS 15163-36-7, Sigma-Aldrich) and 1 mM NADPH at 20 ± 1 °C. Mosquito microsomal membranes were diluted in buffer (0.1 M K_2HPO_4, 0.1 mM EDTA, 1 mM DTT, 5% glycerol pH 7.6), (0.05% bovine serum albumin (BSA), 0.01% zwittergent 3-10) to 0.16 mg/ml corresponding to 4 µg protein per 25 µl enzyme solution. Twenty-five µl enzyme solution and 25 µl substrate solution were incubated for 1 h in a black 384-well plate and the reaction stopped as described above. Each reaction was replicated four times and the fluorescent product HFC was measured at 405 nm while excited at 510 nm. Substrate saturation kinetics were analyzed using GraphPad Prism 8.4 (Michaelis-Menten model).

2.7.2. Microsomal P450 inhibition kinetics

For the determination of IC50-values of different azole compounds and PBO on mosquito (FUMOZ-R) microsomal P450s the probe substrate BOMFC was used at a single concentration around the apparent Km value, i.e. 5 µM (Supplementary Fig. S1), following the general protocol recently described by Haas and Nauen (2021) with minor modifications. The chosen assay conditions were optimized for linearity with time and protein content of 7-hydroxy-4-(trifluoromethyl) coumarin (HC) fluorescent product formation. Microsomes of strain FUMOZ-R were incubated to eleven different concentrations of each inhibitor. Therefore, inhibitors were dissolved in 1:3.3 steps in DMSO at a final concentration of 0.5%, except for epoxiconazole (2%) and uniconazole (1%) to prevent precipitation at the highest concentration. Stock solutions were diluted with 0.1 M potassium-phosphate buffer (pH 7.6) containing 0.01% zwittergent 3-10 (final concentration range between 0.000596 µM and 1, 000 µM). Microsomal preparation was diluted in buffer (0.1 M K_2HPO_4, 0.1 mM EDTA, 1 mM DTT, 5% glycerol, pH 7.6) containing 0.01% zwittergent and 0.05% BSA to 0.16 mg/ml protein corresponding to 4 µg protein/well. Inhibitors and diluted microsomal preparations were applied to a 384-well microplate (384 wells, Greiner bio-one, F-bottom, PS) and incubated for 10 min at 20 ± 1 °C. Subsequently, 25 µl BOMFC/NADPH (final concentration 5 µM/125 µM) solution was added to each well and after 60 min the reaction was stopped as described above. Each reaction was repeated four times. Final assay evaluation was conducted in a microplate reader (Tecan Spark; Excitation: 405 nm; Emission: 510 nm) and reaction mix containing no inhibitor served as full enzyme activity control (100% activity). The controls lacking NADPH and BOMFC were subtracted from each data point. A standard curve was generated using HC to calculate the reaction velocity in pmol HC formed/min × mg protein^{-1}. Data were analysed and IC_{50}-values calculated using a four-parameter non-linear regression fitting routine in GraphPad Prism 8.4.

2.8. RNA extraction and cDNA preparation

RNA was extracted from ten adult female mosquitoes of each strain using TRIzol™ reaction kit following manufacturer's instructions. Afterwards RNA was purified using RNAeasy MINI Kit (Qiagen, Hilden, Germany) following manufacturer's instructions, including a DNAse-digest (RNase-free DNAse Set, 79254, Qiagen, Hilden, Germany) (modifications: Trizol incubation: 10 min, the column containing RNA sample was eluated twice to enhance RNA yields). The RNA concentrations were photometrically determined using 260/280 nm and 230/260 nm ratios (NanoQuant Infinite 200, Tecan, Switzerland). All samples were adjusted to 20 ng/µl.

Afterwards the RNA quality was checked using QIAxcel capillary electrophoresis technology following manufacturer instructions (QIAxcel Advanced, RNA Handbook, Qiagen, Hilden, Germany). RNA cartridge (QIAxcel RNA QC Kit v2.0, ID: 929104) and method CL-RNA were used. QX RNA Size Marker 200–6,000 nt (Qiagen ID: 929580) and QX RNA alignment marker (Qiagen ID: 929510) served as size marker and alignment marker, respectively. Once the RNA quality was confirmed, 0.3 µg of total RNA in 20 µl reaction volume was used for reverse transcription using IScript cDNA synthesis Kit (Bio-Rad, Hercules, USA) following manufacturer's instructions.

2.9. RT-qPCR

RT-qPCR measuring expression levels of CYP6P9a and CYP6P9b was done according to the method recently described by Boaventura et al. (2020) using SsoAdvanced Universal SYBR Green Supermix (Bio-Rad, Hercules, USA) with a total volume of 10 µl using CFX384™ Real-Time system (Bio-Rad, Hercules, USA). Samples were run in triplicate and a non-template control was included as the negative control. Two µl of cDNA with 5 ng/µl and each primer with 200 nM final concentrations were used. The PCR program was as follows: 95 °C for 30 s; 95 °C for 15 s; 55.5 °C for 15 s plate read; steps two and three were repeated 39 times followed by a melting curve from 65 °C to 95 °C in 0.5 °C steps for 5 s. Ribosomal protein S7 (RPS 7) and Actin 5c (Act) served as reference genes in this study. Primer efficiency for each target- and reference gene

was determined in advance with serial 1:5 cDNA dilution and revealed: CYP6P9a: 109.8%; CYP6P9b: 102.8%; Actin 5c: 105.9%; and RPS 7: 104.3%. Stability of the reference genes was checked with Bio-Rad CFX Maestro 1.0 v 4.0 software (Bio-Rad, Hercules, USA) (Vandesompele et al., 2002) and were used for normalization. In this study three to four biological replicates of each strain (FANG and FUMOZ-R) with three technical replicates were measured. Primers and GenBank accession numbers are given in the supplementary information (Supplementary Table S1).

2.10. Statistical analysis

Probit analysis of mosquito bioassay data was performed to calculate LC_{50} values and the 95% confidence intervals using SPSS version 25 (heterogeneity factor 0.5). EC_{50}-values for voltage-gated sodium channel binding of the different pyrethroids were calculated using GraphPad Prism 8.4 (Nonlinear regression, four parameters, variable slope, constraints: bottom: 0, top: 100). Pearson's correlations between mosquito bioassay data and EC_{50}-values were analyzed using GraphPad Prism 8.4. A one-way ANOVA was performed to analyze data for significant differences between data obtained for strains FANG and FUMOZ-R in the biochemical assays. Gene expression analysis was carried out employing Bio-Rad CFX Maestro 1.0 v. 4.0 software (Bio-Rad, Hercules, USA) followed by subsequent unpaired t-tests in qbase (Biogazelle) to compare for significant differences in gene expression levels.

3. Results

3.1. Efficacy of different pyrethroids in glazed tile bioassays

Full dose-response glazed tile bioassays produced a small difference in transfluthrin contact toxicity between *An. funestus* strains FANG and FUMOZ-R, resulting in a resistance ratio (RR) of 2.5 (Table 1). In contrast, FUMOZ-R exhibited high RRs of 223 and 78 against deltamethrin and cypermethrin, respectively. Permethrin and the transfluthrin derivatives TF-0 and TF-1 were the weakest pyrethroids against both strains, with highest LC_{50}-values, as opposed to transfluthrin and its multifluorinated benzyl derivatives TF-3 and TF-5 (Table 1). TF-5 (fenfluthrin) exhibited high contact activity similar to transfluthrin against both strains with a low RR for FUMOZ-R of 1.88, indicating a lack of cross-resistance with deltamethrin and cypermethrin. Based on LC_{50}-values the following efficacy ranking was obtained for the transfluthrin derivatives in glazed tile bioassays with strains FANG and FUMOZ-R: TF = TF-5 > TF-3 >> TF-0 = TF-1 and TF = TF-5 > TF-3 > TF-1 > TF-0, respectively. Those transfluthrin derivatives with a para-fluorinated benzyl ring, TF-1 and TF-5, showed the lowest RRs (< 2) in strain FUMOZ-R, followed by transfluthrin (2.51), TF-0 (3.77) and TF-3 (5.77).

3.2. Sensitivity of recombinantly expressed VGSC to pyrethroids

Pyrethroid activity to *M. domestica* VGSCs heterologously expressed in HEK293 cells was measured by sensing membrane potential changes using fluorescence imaging upon pyrethroid application (Fig. 2). The addition of deltamethrin to HEK293-VGSC cells increased the fluorescence signal in a concentration-dependent manner with an EC_{50}-value of 5.29 nM (95% CI: 4.43–6.30), suggesting high intrinsic VGSC activation (Supplementary Table S2). Cypermethrin and permethrin were significantly less effective and showed EC_{50}-values of 38.9 nM (95% CI: 34.2–44.3) and 721 nM (95% CI: 591–882), respectively (Fig. 2A; Supplementary Table S2). The most potent compound from the transfluthrin series was TF-5 exhibiting an EC_{50}-value similar to permethrin (736 nM (95% CI: 650–834)), followed by transfluthrin, TF-3, TF-1 and TF-0 (Fig. 2B; Supplementary Table S2). The EC_{50}-values of transfluthrin derivatives obtained *in vitro* were strongly correlated with their observed *in vivo* potential in glazed tile bioassays against adult mosquitoes of both strain FANG (Fig. 2C) and FUMOZ-R (Fig. 2D). Such a correlation was also observed for deltamethrin, cypermethrin and permethrin, but only in the pyrethroid susceptible strain FANG (Fig. 2C). In contrast no such correlation was obtained for the resistant strain FUMOZ-R (Fig. 2D). Interestingly transfluthrin and TF-5, despite being more than 100-fold less active on VGSC, exhibited a similar *in vivo* efficacy based on LC_{50}-values in glazed tile bioassays as deltamethrin against strain FANG (Fig. 2C), suggesting additional factors involved in acute contact toxicity than potency on VGSC.

3.3. Synergism of pyrethroid efficacy by different P450 inhibitors

Synergists were first tested for their solo contact toxicity in glazed tile assays to select concentrations not affecting adult survival. At the highest 1-ABT concentration tested (750 mg/m^2), mortality in both strains was < 10%. In contrast PBO and triflumizole were toxic against both strains, but at high concentrations. PBO and triflumizole were more active against the susceptible FANG strain with an LC_{50}-value of 325 mg/m^2 (95% CI: 199–707) and 136 mg/m^2 (95% CI: 40.5–188) respectively. Whereas both synergists were less toxic to the resistant strain FUMOZ-R as demonstrated by LC_{50}-values of > 1,000 mg/m^2 and 392 mg/m^2 (95% CI: 293–508) for PBO and triflumizole respectively. Sublethal concentrations of all synergists applied to glazed tiles were readily taken up after 30 min contact by FUMOZ-R adults as shown by UPLC/MS analysis of legs and body extracts, confirming their internalization (Fig. 3). All synergists were highly effective in strain FUMOZ-R in combination with deltamethrin (Fig. 4). This included both the azole compounds triflumizole and 1-ABT not previously tested for their synergistic potential in *An. funestus*. The synergistic ratios for deltamethrin in strain FUMOZ-R were > 100-fold, whereas permethrin, transfluthrin and derivatives were significantly lower (Fig. 4, Supplementary Table S3). There was minimal

Table 1
Log-dose probit-mortality data (24 h) for different pyrethroids against female adults of *Anopheles funestus* strains FANG and FUMOZ-R in glazed tile bioassays after contact exposure (30 min).

Compound	*An. funestus* FANG (susceptible)					*An. funestus* FUMOZ-R (resistant)					RR
	LC_{50} (mg/m^2)	95% CI	Slope ± SE		*n*	LC_{50} (mg/m^2)	95% CI	Slope ± SE		*n*	
Transfluthrin (TF)	0.023	0.0155–0.0324	1.47	0.168	420	0.0576	0.0191–0.112	1.6	0.218	360	2.51
TF-0	1.19	0.565–1.790	2.90	0.932	140	4.47	2.89–6.01	3.17	0.655	360	3.77
TF-1	1.42	1.02–1.85	2.97	0.453	560	1.41	1.15–1.83	4.79	0.772	350	0.99
TF-3	0.0494	0.0350–0.0664	1.96	0.256	420	0.285	0.225–0.354	3.32	0.495	360	5.77
TF-5	0.0237	0.0132–0.0394	2.03	0.243	420	0.0446	0.0299–0.0592	2.08	0.316	560	1.88
Permethrin	0.543	0.409–0.702	2.28	0.294	420	4.21	2.79–5.88	1.99	0.278	360	7.76
Cypermethrin	0.0968	0.0686–0.1260	2.74	0.479	420	7.54	5.24–10.40	1.86	0.204	540	77.9
Deltamethrin	0.0206	0.0153–0.0273	1.38	0.119	420	4.61	2.73–7.50	1.07	0.102	540	223

Note: Resistance ratio (RR) = LC_{50} FUMOZ-R divided by LC_{50} FANG.
Abbreviation: 95% CI, 95% confidence interval; SE, standard error.

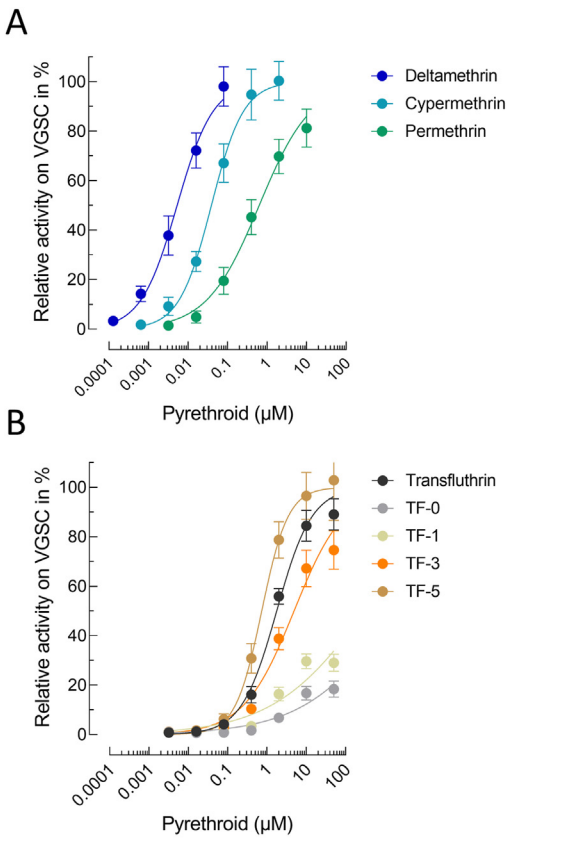

Fig. 2 Concentration response curves for common pyrethroids (**A**) and transfluthrin derivatives (**B**) measured on functionally expressed house fly voltage-gated sodium channels (VGSC) using a fluorescence-based membrane potential cation influx assay. Data are mean values ± standard deviation (SD) (n = 12). **C**, **D** Pearson's correlation analysis between *in vitro* VGSC EC_{50}-values and *in vivo* LC_{50}-values obtained from glazed tile bioassays against female adults of *Anopheles funestus* strains FANG (**C**) and FUMOZ-R (**D**). Data points circled with a dashed line represent deltamethrin, cypermethrin and permethrin.

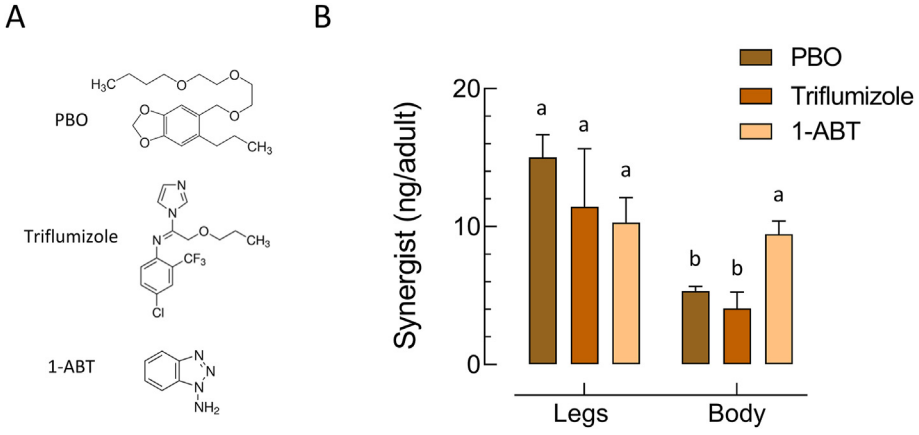

Fig. 3 Tarsal uptake of different synergists by adult females of *Anopheles funestus* strain FUMOZ-R by contact exposure for 30 min on glazed tiles. **A** Three different synergists were tested *in vivo*: piperonyl butoxide (PBO; 100 mg/m^2), triflumizole (100 mg/m^2) and 1-aminobenzotriazole (1-ABT; 250 mg/m^2). **B** Amount of synergist internalized and detected in mosquito legs and bodies analyzed by UPLC/MS. Different letters denote a significant difference (One-way ANOVA, Tukey's *post-hoc* comparisons, $P < 0.05$). Data are mean values ± standard deviation (SD) (n = 20).

synergism of transfluthrin and derivative toxicity in the pyrethroid susceptible strain FANG, whereas moderate synergism was detected for the other pyrethroids - depending on the synergist applied (Supplementary Table S3). The synergistic ratios obtained for the transfluthrin derivatives tested against FUMOZ-R revealed weak or no synergism for TF-1 and TF-5 (Fig. 4), which are fluorinated at the para position of the benzyl ring (Fig. 1). A summary of all bioassay data including 64 calculated LC_{50}-values, resistance factors and synergistic ratios is provided in Supplementary Table S3.

3.4. Activity and inhibition of An. funestus microsomal cytochrome P450 monooxygenases

Microsomal membranes of *An. funestus* strain FUMOZ-R were isolated and tested for their capacity to metabolize a range of different coumarin and resorufin fluorescent probe substrates. The substrate profile obtained for FUMOZ-R microsomes revealed a clear preference for coumarins over resorufins. It is noteworthy that the O-debenzylation of bulkier substrates such as BFC, BOMFC and BOMR was the preferred reaction catalyzed by *An. funestus* microsomal P450s, followed by the O-dealkylation of smaller substrates such as EFC and MFC (Fig. 5). Those substrates showing the highest activity with FUMOZ-R microsomes were also tested with FANG microsomes. As expected, probe activity was consistently lower when compared to FUMOZ-R, consistent with higher P450 activity in the pyrethroid-resistant strain. The most active probe substrate was BOMFC. O-debenzylation by both FANG and FUMOZ-R microsomes followed Michaelis-Menten kinetics with apparent Km- and Vmax-values of 5.76 μM (95% CI: 3.31–9.67) and 21.5 pmol HFC/min/mg protein (95% CI: 18.9–24.4), and 4.41 μM (95% CI: 3.64–5.33) 114 pmol HFC/min/mg protein (95% CI: 109–119), respectively (Supplementary Fig. S1). The

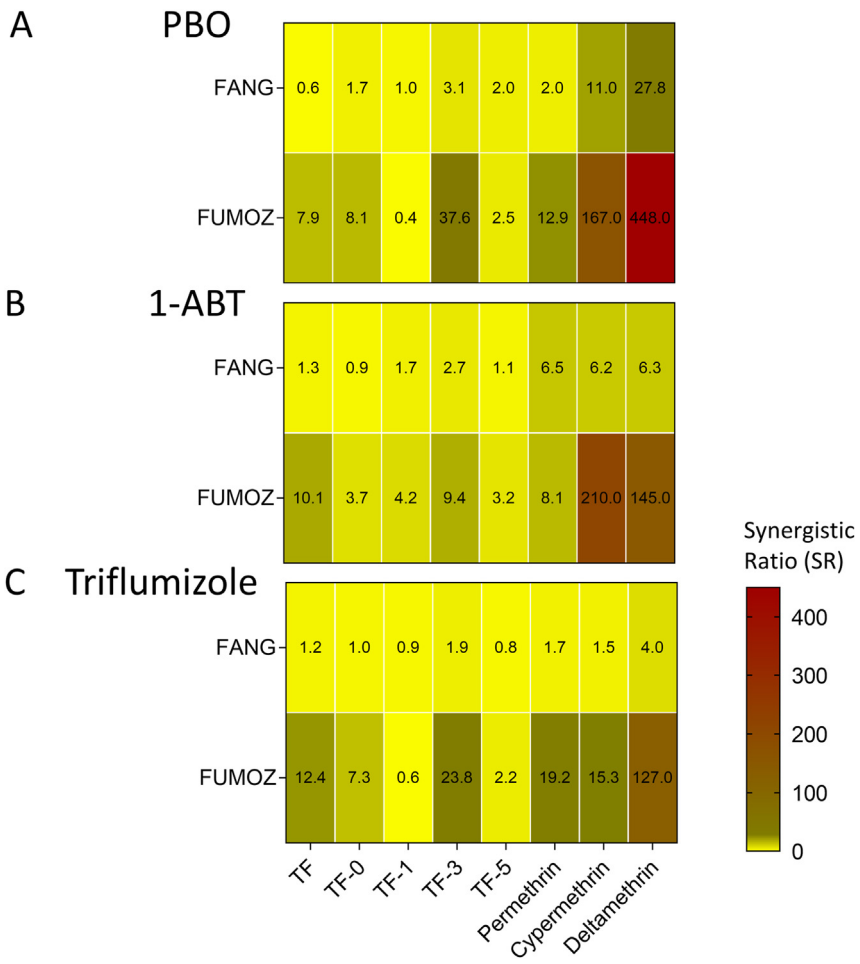

Fig. 4 Heat maps displaying the synergistic ratio obtained in glazed tile bioassays for different pyrethroid insecticides in *Anopheles funestus* strain FANG (susceptible) and FUMOZ-R (resistant) upon contact exposure to piperonyl butoxide (PBO) (**A**), 1-amino-benzotriazole (1-ABT) (**B**) and triflumizole (**C**), directly prior to insecticide application. Synergistic ratios (SR) were calculated by dividing the LC_{50} of the insecticide by the LC_{50} of the insecticide + synergist (see Supplementary Table S3 for details).

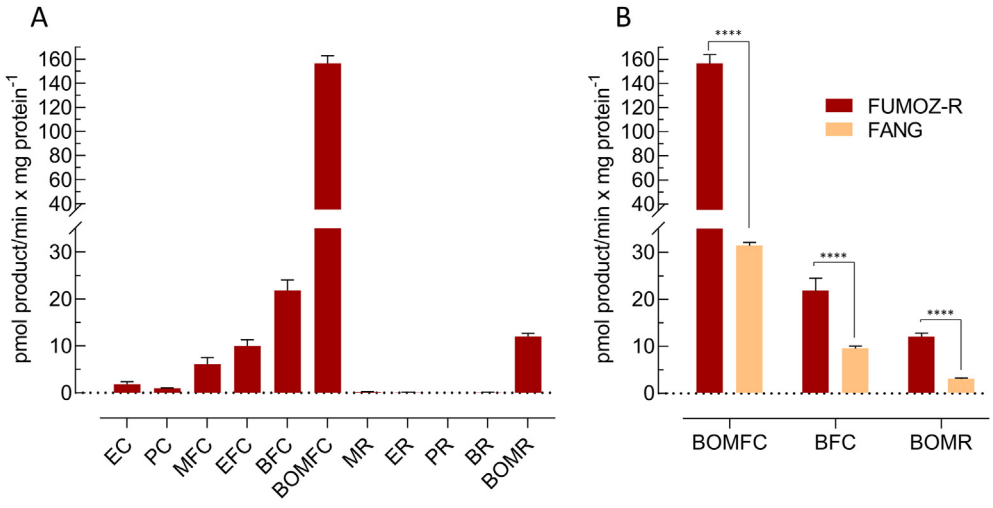

Fig. 5 Metabolism of different cytochrome P450 coumarin and resorufin model substrates by microsomal preparations of *Anopheles funestus*, strain FUMOZ-R (**A**) and strain FANG (**B**) in comparison to FUMOZ-R with those substrates displaying highest cytochrome P450 activity. Data are mean values ± standard deviation (SD) ($n = 4$). Significant differences are denoted by ****$P \leq 0.0001$. *Substrate abbreviations*: EC, 7-ethoxycoumarin; PC, 7-pentoxycoumarin; MFC, 7-methoxy-4-trifluoromethyl coumarin; EFC, 7-ethoxy-4-trifluoromethylcoumarin; BFC, 7-benzyloxy-4-trifluoromethylcoumarin; BOMFC, 7-benzyloxymethoxy-4-trifluoromethylcoumarin; MR, 7-methoxyresorufin; ER, 7-ethoxyresorufin; PR, 7-n-pentoxyresorufin; BR, 7-benzyloxyresorufin ether; BOMR, 7-benzyloxymethoxyresorufin.

significantly higher microsomal BOMFC probe activity of FUMOZ-R compared to FANG was correlated with the overexpression of the well-known P450 variants CYP6P9a and CYP6P9b, as shown by RT-qPCR (Fig. 6).

Using the highly active probe substrate BOMFC we developed a fluorescence-based high-throughput 384-well plate assay allowing us to assess compounds for their potential to inhibit P450 activity in microsomal preparations of *An. funestus* strain FUMOZ-R. PBO is a potent nanomolar P450 inhibitor that is commonly used in products to inhibit P450-based metabolism, whereas azole fungicides are known to act synergistic in combination with certain neonicotinoids and pyrethroids, particularly in honey bees (Iwasa et al., 2004). The azole fungicides prochloraz ($IC_{50} = 5.92$ nM), triflumizole ($IC_{50} = 46.8$ nM), uniconazole ($IC_{50} = 107$ nM) were stronger inhibitors than PBO ($IC_{50} = 260$ nM),

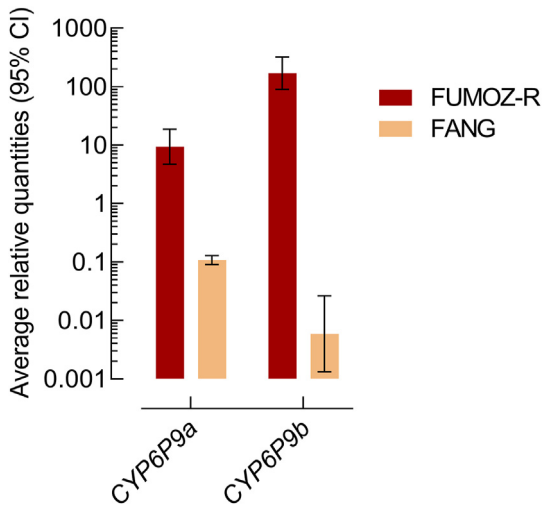

Fig. 6 Expression level (log-scale) of *CYP6P9a* and *CYP6P9b* in *Anopheles funestus* strains FUMOZ-R and FANG measured by qPCR. The expression level was normalized to *RPS7* and *Act* (5c) reference genes. Data are mean values ± 95% CI ($n = 4$ FUMOZ-R and $n = 3$ for FANG).

Table 2
Inhibition of cytochrome P450 activity in microsomal preparations of *Anopheles funestus* FUMOZ-R by different azole fungicides using BOMFC as a substrate. The calculated IC_{50}-values are based on the inhibition of total microsomal monooxygenase activity. Data are mean values ($n = 4$).

Compound	IC_{50} (μM)	95% CI
PBO	0.26	0.221–0.306
1-ABT	119	102–140
Triflumizole	0.0468	0.0416–0.0526
Prochloraz	0.00592	0.00527–0.00664
Uniconazole	0.107	0.0878–0.131
Propiconazole	0.35	0.313–0.39
Epoxiconazole	6.93	5.55–8.71
Triadimefon	1.09	0.967–1.23
Triadimenol	12.3	10.6–14.4
Tebuconazole	0.492	0.444–0.545
Ketoconazole	0.26	0.223–0.302

Abbreviation: 95% CI, 95% confidence interval.

whereas ketoconazole ($IC_{50} = 260$ nM) was similar (Table 2). Interestingly, 1-ABT, a widely known P450 inhibitor, showed a rather weak inhibitory potential ($IC_{50} = 119$ μM), although its synergistic potential *in vivo* in combination with pyrethroids such as deltamethrin against strain FUMOZ-R was comparable to triflumizole and PBO (Supplementary Table S3).

4. Discussion

Based on the lack of synergism with PBO, transfluthrin has been previously described to be less affected than phenoxybenzyl-substituted pyrethroids (e.g. deltamethrin) by P450-mediated metabolic resistance in the *An. funestus* laboratory strain FUMOZ-R (Horstmann and Sonneck, 2016), which has elevated levels of P450 activity driven by CYP6P9a and CYP6P9b (Hunt et al., 2005; Amenya et al., 2008; Coetzee and Koekemoer, 2013; Riveron et al., 2013). This study has confirmed that a very low level of cross-resistance exists between transfluthrin (RR = 2.57), and common pyrethroids such as deltamethrin (RR = 223) and cypermethrin (RR = 77.9) in FUMOZ-R compared to the susceptible strain FANG. The low resistance ratios also extended to other transfluthrin derivatives with varied levels of benzyl fluorination. The surprisingly low level of permethrin resistance in FUMOZ-R is comparable to a RR of 11.49 recently reported by Williams et al. (2019) in tarsal contact (glass plate) bioassays, but in comparison to the insecticide susceptible *An. gambiae* strain Kisumu.

Oxidation of the 4′-position on the phenoxybenzyl ring is one of the primary targets of P450 mediated metabolism of pyrethroids (Shono et al., 1979; Stevenson et al., 2011; Kasai et al., 2014; Zimmer et al., 2014), while other routes of metabolism include the gem dimethyl hydroxylation and an ester- or ether-cleavage (Casida et al., 1983; Weerasinghe et al., 2001; Stevenson et al., 2011). The most active compounds against the resistant FUMOZ-R strain were transfluthrin and TF-5 (fenfluthrin), followed by TF-3, where fluorination of the transfluthrin benzyl ring is expected to offer protection against P450 attack (Horstmann and Sonneck, 2016). However, this does not explain the low resistance ratio for the non-fluorinated TF-0 (RR = 3.77), where other factors may be contributing to reduced P450 metabolism. The most likely explanation is the lack of the 3-phenoxybenzyl moiety, which has been shown to be less susceptible to P450 metabolism in other pyrethroid-resistant insects such cotton bollworm (Tan and McCaffery, 2007) and does not correlate with pyrethroid resistance in house flies (Khan et al., 2017). Furthermore, P450 metabolism of transfluthrin in rats is *via* hydrolysis rather than benzyl ring hydroxylation (Yoshida, 2012, 2013). The RR for permethrin was also *c.*10 to 30-fold lower than for cypermethrin and deltamethrin, respectively. Taken together, this suggests a strong preference for the presence of a 3-phenoxybenzyl moiety and an alpha-cyano group in pyrethroid metabolism by *An. funestus* FUMOZ-R, possibly driven by the extensive use of deltamethrin-treated LLINs for malaria control in Africa that may have applied selective pressure on P450s with an active-site preference for deltamethrin and structurally related pyrethroids.

Pyrethroid resistance in *An. funestus* is strongly linked to the overexpression of CYP6P9a and CYP6P9b that can metabolize deltamethrin and permethrin (Riveron et al, 2013, 2014; Yunta et al., 2019). However, depending on the geographical origin of *An. funestus*, other P450s such as CYP6M7 were also shown to be highly overexpressed and involved in pyrethroid resistance (Riveron et al., 2014). Both CYP6P9a and CYP6P9b were highly expressed in the resistant FUMOZ-R strain relative to the susceptible FANG strain and the lack of cross-resistance with deltamethrin or cypermethrin suggests a limited role in transfluthrin metabolism; however, we did not test the expression level of CYP6M7. Transfluthrin has a 2,3,5,6-tetrafluorobenzyl substitution pattern that leaves the benzyl para-position (4′-position) free for P450 attack. In comparing the synergist ratios of the P450 inhibitors PBO, 1-ABT and triflumizole (Fig. 4) where a high ratio is indicative of P450 metabolism, it was striking that a single fluorination of the 4′-position in TF-1 was equally effective at blocking P450 metabolism as the fully fluorinated TF-5, as evidenced by very low synergist ratios. Whereas transfluthrin, TF-3 and TF-0 produced higher synergist ratios indicative of greater P450 metabolism possibly depending on the halogenation pattern, thus confirming to some extent previous mosquito studies on the importance of the 4′-position for oxidative attack (Horstmann and Sonneck, 2016).

The acute contact toxicity of permethrin against FANG was significantly lower compared to deltamethrin and cypermethrin. Interestingly, transfluthrin, TF-3 and TF-5 were also up-to 25-fold more active than permethrin in glazed tile bioassays against strain FANG, although their intrinsic activity on recombinantly expressed house fly VGSC *in vitro* was not different. Since we had no access to a mosquito VGSC, we employed a surrogate from *M. domestica*, a phylogenetically related dipteran species. Dipteran VGSC proteins show a high level of conservation (Silva and Scott, 2020) and a comparison of important amino acid residues described for pyrethroid binding and known to confer different levels of target-site resistance revealed 100% identity between *An. funestus* (GenBank KY499806.1) and *M. domestica* (GenBank X96668.1) VGSC (O'Reilly et al., 2006; Field et al., 2017). Therefore, the agonistic potency on house fly VGSC obtained here should be a good estimate of intrinsic pyrethroid potency in mosquitoes as well. This assumption is supported by earlier results showing a Kd of 4.7 nM for deltamethrin on *Drosophila* wildtype VGSC functionally expressed in *Xenopus* oocytes (Vais et al., 2003), a value strikingly similar to the EC_{50} of 5.3 nM we measured

(Supplementary Table S2), albeit in a different assay system. Electrophysiological recordings on expressed *Drosophila* para VGSC also revealed weaker activity of permethrin (Warmke et al., 1997), and another study with fenfluthrin (TF-5) on wildtype *Drosophila* VGSC reported a similar action to that for permethrin at low micromolar concentrations (Usherwood et al., 2007), correlating with our finding on house fly VGSC. The discrepancy in VGSC potency between deltamethrin and transfluthrin (and some of its derivatives) did not correlate with their almost identical contact toxicity in glazed tile bioassays and merits further research.

Fluorescent substrates are frequently used to measure P450 activity and could be applied to monitor changes in P450 activity associated with insecticide resistance. The biochemical profiling of resorufins and coumarins against P450-containing microsomes from *An. funestus* FUMOZ-R showed a strong preference for BOMFC, BFC and BOMR, all bulky substrates substituted with a benzyloxy-group. These were rapidly O-debenzylated to provide a robust and reliable fluorescence read-out through conversion to umbelliferone. A similar substrate preference has been described for CYP6BQ9 and CYP6BQ23 that are also associated with pyrethroid resistance in *Tribolium castaneum* and *Meligethes aeneus*, respectively (Zhu et al., 2010; Zimmer et al., 2014). Resorufin ether substrates have been used with mixed success, being suitable as substrate probes for *An. gambiae* CYP6M2, CYP6Z2 and CYP6P3, but unreactive against pyrethroid metabolising *Aedes aegypti* P450s. However, BOMR to the best of our knowledge was not included in previous studies with malaria vectors, though alternative resorufin substrates were described in combination with CYP6P9-variants (Ibrahim et al., 2015, 2016). In comparison with resorufin, the coumarin based substrates produced much stronger fluorescence signals (Fig. 5). BOMFC produced the highest fluorescence activity suggesting that this probe substrate could be applied to biochemically profile P450 activity in mosquito populations. This is supported by the fact that microsomal membrane preparations of strain FUMOZ-R were significantly more active with BOMFC than those of strain FANG. Considering the upregulation of CYP6P9a and CYP6P9b in strain FUMOZ-R tested here, it is likely that these P450s are contributing to BOMFC O-debenzylation and hydroxycoumarin formation, although we cannot exclude a potential role of other P450s.

We have used BOMFC to develop a biochemical microplate (384 wells) assay to screen the inhibitory potential of a range of azole compounds with *An. funestus* microsomal P450s. The assay is largely based on a recently described mechanistic bee pollinator risk assessment approach to assess pesticide synergism issues in honey bees (Haas and Nauen, 2021). Synergistic effects of azole fungicides in combination with pyrethroids and neonicotinoids, respectively, have been described in honey bees at the phenotypic level (Pilling and Jepson, 1993; Iwasa et al., 2004), but were only recently deciphered at the molecular level (Haas and Nauen, 2021). Here, we identified prochloraz and triflumizole as extremely potent nanomolar inhibitors of microsomal P450s of *An. funestus*, and at least for triflumizole we could confirm its synergistic potential in combination with 3-phenoxybenzyl pyrethroids against FUMOZ-R *in vivo*. Quite surprising was the rather low inhibitory potential of the triazole 1-ABT, a well-known pan-specific P450 inhibitor (Ortiz De Montellano, 2018). Despite its weak inhibition of FUMOZ-R microsomal P450s *in vitro* it was highly active in glazed tile bioassays, e.g. in combination with cypermethrin. However, future work is needed to further investigate the basis of the contrasting results. It would also be interesting to assess the efficacy of triflumizole and other azole compounds against functionally expressed *An. funestus* P450s such as CYP6P9a and CYP6P9b. McLaughlin et al. (2008) tested several drugs for their inhibitory action on the O-debenzylation of benzyloxy-resorufin by *An. gambiae* CYP6Z2, including clotrimazole and ketoconazole, but IC_{50} values were in the micromolar range and no *in vivo* synergist trials were conducted. Here we demonstrated that azole compounds such as triflumizole could serve as an alternative to PBO, known for its synergistic potential against pyrethroid-resistant mosquitoes. Our results would be a good starting point to foster additional studies on the potential of azoles as synergists to overcome P450-mediated pyrethroid resistance in anopheline mosquitoes.

5. Conclusions

The progress in malaria reduction since the turn of millennium has largely stagnated since 2015 with mosquito resistance to pyrethroids that are commonly used in vector control tools such as IRS and ITNs being a threat to the goal of eradicating malaria by 2040 (https://zeroby40.com/). For sustainable vector control interventions, it is therefore important to implement resistance management strategies that are based on the most active molecules available from chemical classes with the same mode of action. Such molecules may not necessarily break but could substantially delay resistance. The pyrethroids most often used in vector control possess the common structural motif of a phenoxybenzyl alcohol coupled with a cyclopropane ring with cross-resistance trends detectable across pyrethroid-resistant populations of *An. funestus*, *An. gambiae*, *An. arabiensis* and *An. coluzzii* (Moyes et al., 2021). It has been suggested that pyrethroid cross-resistance might be mitigated by employing structurally diverse pyrethroids such as bifenthrin (Moyes et al., 2021) and transfluthrin (Horstmann and Sonneck, 2016). Here, we provide further evidence that multifluorinated benzyl pyrethroids offer potential resistance breaking properties against P450-driven pyrethroid resistance in *An. funestus* that require further verification in resistant field populations. Since pyrethroid resistance in *An. funestus* field strains is largely driven by P450-mediated detoxification, we think that the findings presented here on transfluthrin and pyrethroid synergism are highly relevant for applied field conditions. Furthermore, we have expanded the vector control research toolbox by the introduction of a sensitive fluorescent probe substrate BOMFC for the biochemical monitoring of P450-mediated resistance, and the identification of azoles such as triflumizole as new compounds with potential to synergize pyrethroid toxicity in *An. funestus* FUMOZ-R.

Funding

The work was funded by the Innovative Vector Control Consortium (IVCC) and Bayer AG.

CRediT author statement

Melanie Nolden: Methodology, Investigation, Visualization, Formal analysis, Writing - Original draft preparation. Andreas Brockmann: Methodology, Investigation, Formal Analysis. Ulrich Ebbinghaus-Kintscher: Methodology, Writing - Reviewing and Editing. Kai-Uwe Brueggen: Funding acquisition. Sebastian Horstmann: Supervision, Funding acquisition, Writing - Reviewing and Editing. Mark Paine: Supervision, Writing - Reviewing and Editing. Ralf Nauen: Conceptualization, Supervision, Visualization, Writing - Reviewing and Editing.

Declaration of competing interests

The authors declare the following financial interests/personal relationships which may be considered as potential competing interests: Andreas Brockmann, Kai-Uwe Brüggen, Ralf Nauen, Sebastian Horstmann and Ulrich Ebbinghaus-Kintscher are employed by Bayer AG, a manufacturer of pesticides. Melanie Nolden is a PhD student affiliated with the LSTM and funded by the Innovative Vector Control Consortium (IVCC) and Bayer AG. Mark Paine declares that he has no known competing financial interests or personal relationships that could have appeared to influence the work reported in this paper.

Acknowledgements

We are grateful to Joerg Egger and Frederik Kaeding (Bayer Environmental Science) who reared and provided the mosquito strains.

Thanks to Bettina Lueke for the introduction and helpful advice on the biochemical work. We would also like to thank Johannes Glaubitz and Birgit Nebelsiek for analytical support.

Appendix A. Supplementary data

Supplementary data to this article can be found online at https://doi.org/10.1016/j.crpvbd.2021.100041.

References

Abbott, W.S., 1925. A method of computing the effectiveness of an insecticide. J. Econ. Entomol. 18, 265–267.

Amenya, D.A., Naguran, R., Lo, T.-C.M., Ranson, H., Spillings, B.L., Wood, O.R., et al., 2008. Over expression of a cytochrome P450 (CYP6P9) in a major African malaria vector. Insect Mol. Biol. 17, 19–25.

Balabanidou, V., Grigoraki, L., Vontas, J., 2018. Insect cuticle: a critical determinant of insecticide resistance. Curr. Opin. Insect Sci. 27, 68–74.

Behrenz, W., Elbert, A., 1985. Cyfluthrin and fenfluthrin, two new pyrethroidsfor the control of hygiene pests. Anzeiger für Schädlingskunde, Pflanzenschutz. Umweltschutz 58, 30–35.

Bhatt, S., Weiss, D.J., Cameron, E., Bisanzio, D., Mappin, B., Dalrymple, U., et al., 2015. The effect of malaria control on *Plasmodium falciparum* in Africa between 2000 and 2015. Nature 526, 207–211.

Bibbs, C.S., Tsikolia, M., Bloomquist, J.R., Bernier, U.R., De Xue, R., Kaufman, P.E., 2018. Vapor toxicity of five volatile pyrethroids against *Aedes aegypti*, *Aedes albopictus*, *Culex quinquefasciatus*, and *Anopheles quadrimaculatus* (Diptera: Culicidae). Pest Manag. Sci. 74, 2699–2706.

Boaventura, D., Ulrich, J., Lueke, B., Bolzan, A., Okuma, D., Gutbrod, O., et al., 2020. Molecular characterization of Cry1F resistance in fall armyworm, *Spodoptera frugiperda* from Brazil. Insect Biochem. Mol. Biol. 116, 103280.

Bradford, M.M., 1976. A rapid and sensitive method for the quantitation microgram quantities of protein utilizing the principle of protein-dye binding. Anal Biochem 72, 248–254.

Brooke, B.D., Kloke, G., Hunt, R.H., Koekemoer, L.L., Tem, E.A., Taylor, M.E., et al., 2001. Bioassay and biochemical analyses of insecticide resistance in southern African *Anopheles funestus* (Diptera: Culicidae). Bull. Entomol. Res. 91, 265–272.

Casida, J.E., Gammon, D.W., Glickman, A.H., Lawrence, L.J., 1983. Mechanism of selective action of pyrethroid. Annu. Rev. Pharmacol. Toxicol. 413–438.

Coetzee, M., Koekemoer, L.L., 2013. Molecular systematics and insecticide resistance in the major African malaria vector *Anopheles funestus*. Annu. Rev. Entomol. 58, 393–412.

Coleman, M., Hemingway, J., Gleave, K.A., Wiebe, A., Gething, P.W., Moyes, C.L., 2017. Developing global maps of insecticide resistance risk to improve vector control. Malar. J. 16, 86.

Cuamba, N., Morgan, J.C., Irving, H., Steven, A., Wondji, C.S., 2010. High level of pyrethroid resistance in an *Anopheles funestus* population of the Chokwe district in Mozambique. PloS One 5, e11010.

Das, S., Garver, L., Dimopoulos, G., 2007. Protocol for mosquito rearing (*A. gambiae*). JoVE 5, 221.

Davies, T.G.E., Field, L.M., Usherwood, P.N.R., Williamson, M.S., 2007. A comparative study of voltage-gated sodium channels in the Insecta: implications for pyrethroid resistance in Anophelinae and other Neopteran species. Insect Mol. Biol. 16, 361–375.

Djouaka, R., Riveron, J.M., Yessoufou, A., Tchigossou, G., Akoton, R., Irving, H., et al., 2016. Multiple insecticide resistance in an infected population of the malaria vector *Anopheles funestus* in Benin. Parasit. Vectors 9, 453.

Feyereisen, R., 1999. Insect P450 enzymes. Annu. Rev. Entomol. 44, 507–533.

Field, L.M., Emyr Davies, T.G., O'Reilly, A.O., Williamson, M.S., Wallace, B.A., 2017. Voltage-gated sodium channels as targets for pyrethroid insecticides. Eur. Biophys. J. 46, 675–679.

Fongnikin, A., Houeto, N., Agbevo, A., Odjo, A., Syme, T., N'Guessan, R., Ngufor, C., 2020. Efficacy of Fludora® Fusion (a mixture of deltamethrin and clothianidin) for indoor residual spraying against pyrethroid-resistant malaria vectors: laboratory and experimental hut evaluation. Parasit. Vectors 13, 466.

Fuseini, G., Phiri, W.P., von Fricken, M.E., Smith, J., Garcia, G.A., 2019. Evaluation of the residual effectiveness of FludoraTM fusion WP-SB, a combination of clothianidin and deltamethrin, for the control of pyrethroid-resistant malaria vectors on Bioko Island, Equatorial Guinea. Acta Trop. 196, 42–47.

Gleave, K., Lissenden, N., Richardson, M., Ranson, H., 2018. Piperonyl butoxide (PBO) combined with pyrethroids in long-lasting insecticidal nets (LLINs) to prevent malaria in Africa. Cochrane Database Syst. Rev. 11, CD012776. https://doi.org/10.1002/14651858.CD012776.pub2.

Haas, J., Nauen, R., 2021. Pesticide risk assessment at the molecular level using honey bee cytochrome P450 enzymes: a complementary approach. Environ. Int. 147, 106372.

Hargreaves, K., Koekemoer, L.L., Brooke, B.D., Hunt, R.H., Mthembu, J., Coetzee, M., 2000. *Anopheles funestus* resistant to pyrethroid insecticides in South Africa. Med. Vet. Entomol. 14, 181–189.

Hemingway, J., 2019. Malaria parasite tackled in mosquitoes. Nature 567, 185–186.

Hemingway, J., Beaty, B.J., Rowland, M., Scott, T.W., Sharp, B.L., 2006. The Innovative Vector Control Consortium: improved control of mosquito-borne diseases. Trends Parasitol. 22, 308–312.

Hemingway, J., Hawkes, N.J., McCarroll, L., Ranson, H., 2004. The molecular basis of insecticide resistance in mosquitoes. Insect Biochem. Mol. Biol. 34, 653–665.

Hemingway, J., Ranson, H., Magill, A., Kolaczinski, J., Fornadel, C., Gimnig, J., et al., 2016. Averting a malaria disaster: will insecticide resistance derail malaria control? Lancet 387, 1785–1788.

Hoppé, M., Hueter, O.F., Bywater, A., Wege, P., Maienfisch, P., 2016. Evaluation of commercial agrochemicals as new tools for malaria vector control. Chimia 70, 721–729.

Horstmann, S., Sonneck, R., 2016. Contact bioassays with phenoxybenzyl and tetrafluorobenzyl pyrethroids against target-site and metabolic resistant mosquitoes. PloS One 11, e0149738.

Human Disease Vectors (HDV) group of the Insect Pest Control Laboratory, 2017. Guidelines for standardised mass rearing of *Anopheles* mosquitoes.

Hunt, R.H., Brooke, B.D., Pillay, C., Koekemoer, L.L., Coetzee, M., 2005. Laboratory selection for and characteristics of pyrethroid resistance in the malaria vector *Anopheles funestus*. Med. Vet. Entomol. 19, 271–275.

Ibrahim, S.S., Ndula, M., Riveron, J.M., Irving, H., Wondji, C.S., 2016. The P450 CYP6Z1 confers carbamate/pyrethroid cross-resistance in a major African malaria vector beside a novel carbamate-insensitive N485I acetylcholinesterase-1 mutation. Mol. Ecol. 25, 3436–3452.

Ibrahim, S.S., Riveron, J.M., Bibby, J., Irving, H., Yunta, C., Paine, M.J.I., Wondji, C.S., 2015. Allelic variation of cytochrome P450s drives resistance to bednet insecticides in a major malaria vector. PLoS Genet. 11, e1005618.

Irving, H., Riveron, J.M., Ibrahim, S.S., Lobo, N.F., Wondji, C.S., 2012. Positional cloning of rp2 QTL associates the P450 genes CYP6Z1, CYP6Z3 and CYP6M7 with pyrethroid resistance in the malaria vector *Anopheles funestus*. Heredity 109, 383–392.

Irving, H., Wondji, C.S., 2017. Investigating knockdown resistance (kdr) mechanism against pyrethroids/DDT in the malaria vector *Anopheles funestus* across Africa. BMC Genet. 18, 76.

Iwasa, T., Motoyama, N., Ambrose, J.T., Roe, R.M., 2004. Mechanism for the differential toxicity of neonicotinoid insecticides in the honey bee, *Apis mellifera*. Crop Protect. 23, 371–378.

Kasai, S., Komagata, O., Itokawa, K., Shono, T., Ng, L.C., Kobayashi, M., Tomita, T., 2014. Mechanisms of pyrethroid resistance in the dengue mosquito vector, *Aedes aegypti*: target site insensitivity, penetration, and metabolism. PLoS Negl. Trop. Dis. 8, e2948.

Khan, H.A.A., Akram, W., Fatima, A., 2017. Resistance to pyrethroid insecticides in house flies, *Musca domestica* L. (Diptera: Muscidae) collected from urban areas in Punjab, Pakistan. Parasitol. Res. 116, 3381–3385.

Kline, D.L., Urban, J., 2018. Potential for utilization of spatial repellents in mosquito control interventions. ACS Symp. Ser. 1289, 237–248.

Laufer, J., Rochet, M., Pelhate, M., Elliotti, M., Janes, N.F., Sattelle, D.B., 1984. Pyrethroids insecticides: actions of deltamethrin and related compounds on insect axonal sodium channels. J. Insect Physiol. 30, 341–349.

Manjon, C., Troczka, B.J., Zaworra, M., Beadle, K., Randall, E., Hertlein, G., et al., 2018. Unravelling the molecular determinants of bee sensitivity to neonicotinoid insecticides. Curr. Biol. 28, 1137–1143.

Masalu, J.P., Finda, M., Killeen, G.F., Ngowo, H.S., Pinda, P.G., Okumu, F.O., 2020. Creating mosquito-free outdoor spaces using transfluthrin-treated chairs and ribbons. Malar. J. 19, 109.

McLaughlin, L.A., Niazi, U., Bibby, J., David, J.P., Vontas, J., Hemingway, J., et al., 2008. Characterization of inhibitors and substrates of *Anopheles gambiae* CYP6Z2. Insect Mol. Biol. 17, 125–135.

Morgan, J.C., Irving, H., Okedi, L.M., Steven, A., Wondji, C.S., 2010. Pyrethroid resistance in an *Anopheles funestus* population from Uganda. PloS One 5, e11872.

Moyes, C.L., Athinya, D.K., Seethaler, T., Battle, K.E., Sinka, M., Hadi, M.P., et al., 2020. Evaluating insecticide resistance across African districts to aid malaria control decisions. Proc. Natl. Acad. Sci. U.S.A. 117, 202006781.

Nauen, R., 2007. Insecticide resistance in disease vectors of public health importance. Pest Manag. Sci. 63, 628–633.

Moyes, C.L., Lees, R.S., Yunta, C., Walker, K.J., Hemmings, K., Oladepo, F., et al., 2021. Assessing cross-resistance within the pyrethroids in terms of their interactions with key cytochrome P450 enzymes and resistance in vector populations. Parasit. Vectors 14, 115.

Nauen, R., 2006. Insecticide mode of action: return of the ryanodine receptor. Pest Manag. Sci. 62, 690–692.

Naumann, K., 1990. Synthetic pyrethroid insecticides: formation of the pyrethroid-ester-linkage, chemistry and patents. In: Chemistry of Plant Protection, vol. 5. Springer-Verlag, Weinheim, pp. 129–173.

Ogoma, S.B., Ngonyani, H., Simfukwe, E.T., Mseka, A., Moore, J., Killeen, G.F., 2012. Spatial repellency of transfluthrin-treated hessian strips against laboratory-reared *Anopheles arabiensis* mosquitoes in a semi-field tunnel cage. Parasit. Vectors 5, 54.

Ogoma, S.B., Ngonyani, H., Simfukwe, E.T., Mseka, A., Moore, J., Maia, M.F., et al., 2014. The mode of action of spatial repellents and their impact on vectorial capacity of *Anopheles gambiae sensu stricto*. PloS One 9, e110433.

O'Reilly, A.O., Khambay, B.P.S., Williamson, M.S., Field, L.M., Wallace, B.A., Davies, T.G.E., 2006. Modelling insecticide-binding sites in the voltage-gated sodium channel. Biochem. J. 396, 255–263.

Ortiz De Montellano, P.R., 2018. 1-Aminobenzotriazole: a mechanism-based cytochrome P450 inhibitor and probe of cytochrome P450 biology. Med. Chem. 8, 038.

Pilling, E.D., Jepson, P.C., 1993. Synergism between EBI fungicides and a pyrethroid insecticide in the honey bee (*Apis mellifera*). Pestic. Sci. 39, 293–297.

Pulman, D.A., 2011. Deltamethrin: the cream of the crop. J. Agric. Food. Chem. 59, 2770–2772.

Riveron, J.M., Ibrahim, S.S., Chanda, E., Mzilahowa, T., Cuamba, N., Irving, H., et al., 2014. The highly polymorphic CYP6M7 cytochrome P450 gene partners with the directionally selected CYP6P9a and CYP6P9b genes to expand the pyrethroid

resistance front in the malaria vector *Anopheles funestus* in Africa. BMC Genomics 15, 817.
Riveron, J.M., Irving, H., Ndula, M., Barnes, K.G., Ibrahim, S.S., Paine, M.J.I., Wondji, C.S., 2013. Directionally selected cytochrome P450 alleles are driving the spread of pyrethroid resistance in the major malaria vector *Anopheles funestus*. Proc. Natl. Acad. Sci. U.S.A. 110, 252–257.
Sangba, M.L.O., Deketramete, T., Wango, S.P., Kazanji, M., Akogbeto, M., Ndiath, M.O., 2016. Insecticide resistance status of the *Anopheles funestus* population in Central African Republic: a challenge in the war. Parasit. Vectors 9, 230.
Scott, J.G., 2019. Life and death at the voltage-sensitive sodium channel: evolution in response to insecticide use. Annu. Rev. Entomol. 64, 243–257.
Shono, T., Ohsawa, K., Casida, J.E., 1979. Metabolism of trans-and cis-permethrin, trans- and cis-cypermethrin, and decamethrin by microsomal enzymes. J. Agric. Food. Chem. 27, 316–325.
Silva, J.J., Scott, J.G., 2020. Conservation of the voltage-sensitive sodium channel protein within the Insecta. Insect Mol. Biol. 29, 9–18.
Sinka, M.E., Bangs, M.J., Manguin, S., Coetzee, M., Mbogo, C.M., Hemingway, J., et al., 2010. The dominant *Anopheles* vectors of human malaria in Africa, Europe and the Middle East: occurrence data, distribution maps and bionomic précis. Parasit. Vectors 3, 117.
Sinka, M.E., Golding, N., Massey, N.C., Wiebe, A., Huang, Z., Hay, S.I., Moyes, C.L., 2016. Modelling the relative abundance of the primary African vectors of malaria before and after the implementation of indoor, insecticide-based vector control. Malar. J. 15, 142.
Smith, L.B., Sears, C., Sun, H., Mertz, R.W., Kasai, S., Scott, J.G., 2019. CYP-mediated resistance and cross-resistance to pyrethroids and organophosphates in *Aedes aegypti* in the presence and absence of kdr. Pestic. Biochem. Physiol. 160, 119–126.
Soderlund, D.M., 2020. Neurotoxicology of pyrethroid insecticides. In: Neurotoxicity of pesticides. Elsevier, Amsterdam, pp. 113–165.
Soderlund, D.M., Bloomquist, J.R., 1989. Neurotoxic actions of pyrethroid insecticides. Annu. Rev. Entomol. 34, 77–96.
Sparks, T.C., Nauen, R., 2015. IRAC: mode of action classification and insecticide resistance management. Pestic. Biochem. Physiol. 121, 122–128.
Stevenson, B.J., Bibby, J., Pignatelli, P., Muangnoicharoen, S., O'Neill, P.M., Lian, L.Y., et al., 2011. Cytochrome P450 6M2 from the malaria vector *Anopheles gambiae* metabolizes pyrethroids: sequential metabolism of deltamethrin revealed. Insect Biochem. Mol. Biol. 41, 492–502.
Tan, J., McCaffery, A.R., 2007. Efficacy of various pyrethroid structures against a highly metabolically resistant isogenic strain of *Helicoverpa armigera* (Lepidoptera: Noctuidae) from China. Pest Manag. Sci. 63, 960–968.
Tay, B., Stewart, T.A., Davis, F.M., Deuis, J.R., Vetter, I., 2019. Development of a high-throughput fluorescent no-wash sodium influx assay. PloS One 14, e0213751.
Tchigossou, G., Djouaka, R., Akoton, R., Riveron, J.M., Irving, H., Atoyebi, S., et al., 2018. Molecular basis of permethrin and DDT resistance in an *Anopheles funestus* population from Benin. Parasit. Vectors 11, 602.
Temu, E.A., Minjas, J.N., Tuno, N., Kawada, H., Takagi, M., 2007. Identification of four members of the *Anopheles funestus* (Diptera: Culicidae) group and their role in *Plasmodium falciparum* transmission in Bagamoyo coastal Tanzania. Acta Trop. 102, 119–125.
Ullrich, V., Weber, P., 1972. The O-dealkylation of 7-ethoxycoumarin by liver microsomes. Hoppe. Seylers. Z. Physiol. Chem. 353, 1171–1177.
Usherwood, P.N.R., Davies, T.G.E., Mellor, I.R., O'Reilly, A.O., Peng, F., Vais, H., et al., 2007. Mutations in DIIS5 and the DIIS4-S5 linker of *Drosophila melanogaster* sodium channel define binding domains for pyrethroids and DDT. FEBS Lett. 581, 5485–5492.
Vais, H., Atkinson, S., Pluteanu, F., Goodson, S.J., Devonshire, A.L., Williamson, M.S., Usherwood, P.N.R., 2003. Mutations of the para sodium channel of *Drosophila melanogaster* identify putative binding sites for pyrethroids. Mol. Pharmacol. 64, 914–922.
Vandesompele, J., De Preter, K., Pattyn, F., Poppe, B., Van Roy, N., De Paepe, A., Speleman, F., 2002. Accurate normalization of real-time quantitative RT-PCR data by geometric averaging of multiple internal control genes. Genome Biol. 3, 7.
Vontas, J., Katsavou, E., Mavridis, K., 2020. Cytochrome P450-based metabolic insecticide resistance in *Anopheles* and *Aedes* mosquito vectors: muddying the waters. Pestic. Biochem. Physiol. 170, 104666.
Warmke, J.W., Reenan, R.A.G., Wang, P., Qian, S., Arena, J.P., Wang, J., et al., 1997. Functional expression of *Drosophila* para sodium channels modulation by the membrane protein tipE and toxin pharmacology. J. Gen. Physiol. 110, 119–133.
Weedall, G.D., Mugenzi, L.M.J., Menze, B.D., Tchouakui, M., Ibrahim, S.S., Amvongo-Adjia, N., et al., 2019. A cytochrome P450 allele confers pyrethroid resistance on a major African malaria vector, reducing insecticide-treated bednet efficacy. Sci. Transl. Med. 11, eaat7386.
Weerasinghe, I.S., Kasai, S., Shono, T., 2001. Correlation of pyrethroid structure and resistance level in *Culex quinquefasciatus* Say from Saudi Arabia. J. Pestic. Sci. 26, 158–161.
WHO, 2018a. World malaria report 2018. World Health Organization, Geneva. https://www.who.int/publications/i/item/9789241565653.
WHO, 2018b. Global report on insecticide resistance in malaria vectors: 2010–2016. World Health Organization, Geneva. https://apps.who.int/iris/handle/10665/272533.
Wiebe, A., Longbottom, J., Gleave, K., Shearer, F.M., Sinka, M.E., Massey, N.C., et al., 2017. Geographical distributions of African malaria vector sibling species and evidence for insecticide resistance. Malar. J. 16, 85.
Williams, J., Flood, L., Praulins, G., Ingham, V.A., Morgan, J., Lees, R.S., Ranson, H., 2019. Characterisation of *Anopheles* strains used for laboratory screening of new vector control products. Parasit. Vectors 12, 522.
Wondji, C.S., Irving, H., Morgan, J., Lobo, N.F., Collins, F.H., Hunt, R.H., et al., 2009. Two duplicated P450 genes are associated with pyrethroid resistance in *Anopheles funestus*, a major malaria vector. Genome Res. 19, 452–459.
Yoshida, T., 2013. Analytical method for urinary metabolites of the fluorine-containing pyrethroids metofluthrin , profluthrin and transfluthrin by gas chromatography/mass spectrometry. J Chromatogr B 913–914, 77–83.
Wood, O.R., Hanrahan, S., Coetzee, M., Koekemoer, L.L., Brooke, B.D., 2010. Cuticle thickening associated with pyrethroid resistance in the major malaria vector *Anopheles funestus*. Parasit. Vectors 3, 67.
Yoshida, T., 2012. Identification of urinary metabolites in rats administered the fluorine-containing pyrethroids metofluthrin, profluthrin, and transfluthrin. Toxicol. Environ. Chem. 94, 1789–1804.
Yunta, C., Hemmings, K., Stevenson, B., Koekemoer, L.L., Matambo, T., Pignatelli, P., et al., 2019. Cross-resistance profiles of malaria mosquito P450s associated with pyrethroid resistance against WHO insecticides. Pestic. Biochem. Physiol. 161, 61–67.
Zaworra, M., Nauen, R., 2019. New approaches to old problems: removal of phospholipase A2 results in highly active microsomal membranes from the honey bee, *Apis mellifera*. Pestic. Biochem. Physiol. 161, 68–76.
Zhu, F., Parthasarathy, R., Bai, H., Woithe, K., Kaussmann, M., Nauen, R., et al., 2010. A brain-specific cytochrome P450 responsible for the majority of deltamethrin resistance in the QTC279 strain of *Tribolium castaneum*. Proc. Natl. Acad. Sci. U.S.A. 107, 8557–8562.
Zimmer, C.T., Bass, C., Williamson, M.S., Kaussmann, M., Wölfel, K., Gutbrod, O., Nauen, R., 2014. Molecular and functional characterization of CYP6BQ23, a cytochrome P450 conferring resistance to pyrethroids in European populations of pollen beetle, *Meligethes aeneus*. Insect Biochem. Mol. Biol. 45, 18–29.